ENTROPY SOLUTIONS OF A SCALAR CONSERVATION LAW MODELLING SEDIMENTATION IN VESSELS WITH VARYING CROSS-SECTIONAL AREA*

RAIMUND BÜRGER†, JULIO CAREAGA†, AND STEFAN DIEHL‡

Abstract. The sedimentation of an ideal suspension in a vessel with variable cross-sectional area can be described by an initial-boundary value problem for a scalar nonlinear hyperbolic conservation law with a nonconvex flux function and a weight function that depends on spatial position. The sought unknown is the local solids volume fraction. For the most important cases of vessels with downward-decreasing cross-sectional area and flux function with at most one inflection point, entropy solutions of this problem are constructed by the method of characteristics. Solutions exhibit discontinuities that mostly travel at variable speed, i.e., they are curved in the space-time plane. These trajectories are given by ordinary differential equations that arise from the jump condition. It is shown that three qualitatively different solutions may occur in dependence of the initial concentration. The potential application of the findings is a new method of flux identification via settling tests in a suitably shaped vessel. Related models also arise in flows of vehicular traffic, pedestrians, and in pipes with varying cross-sectional area.

Key words. conservation law, method of characteristics, shock wave, variable cross-section

AMS subject classifications. 35L65, 76T20, 76M99

1. Introduction.

1.1. Scope. The sedimentation of solid particles in a liquid in a closed vessel can be modelled by the following initial-boundary value problem for a scalar nonlinear hyperbolic conservation law:

$$\partial_t\big(A(x)\phi\big) - \partial_x\big(A(x)f(\phi)\big) = 0 \qquad \text{for } 0 < x < 1,\ t > 0, \tag{1a}$$

$$\phi(x,0) = \phi_0 \qquad \text{for } 0 < x < 1, \tag{1b}$$

$$\phi(0^+,t) = \phi_{\max} \quad \text{and} \quad \phi(1^-,t) = 0 \qquad \text{for } t > 0. \tag{1c}$$

The local solids volume fraction $\phi(x,t)$ is the sought function, which is constant ϕ_0 initially and $\phi_{\max}$ at the bottom $x = 0$, where $\phi_{\max}$ is a maximum packing volume fraction. The cross-sectional area $A = A(x) \in C^1$ is a given function of the height x, and the nonlinear flux function $f = f(\phi)$ models hindered settling by gravity according to the kinematic sedimentation theory by Kynch [22]. This theory is based on the assumption that the solids batch settling velocity is a function of ϕ. This assumption is valid only for solid mono-sized particles such as glass beads, but it is widely applied to other materials, and in particular to the dilute regime of flocculated suspensions in mineral processing and wastewater treatment [9, 10, 18].

Knowledge of f for given solid and liquid materials is fundamental for the description, simulation and control of batch and continuous sedimentation in these and other applications. A simple test that exhibits a rich solution behaviour, and thereby

*This work was funded by CONICYT (Chile) through projects Fondecyt 1130154; BASAL project CMM, Universidad de Chile and Centro de Investigación en Ingeniería Matemática (CI^{2}MA), Universidad de Concepción; Anillo ACT1118 (ANANUM); CRHIAM, project CONICYT/FONDAP/15130015; and Fondef ID15I10291.

†CI^{2}MA and Departamento de Ingeniería Matemática, Facultad de Ciencias Físicas y Matemáticas, Universidad de Concepción, Casilla 160-C, Concepción, Chile (rburger@ing-mat.udec.cl), (juliocareaga@udec.cl)

‡Centre for Mathematical Sciences, Lund University, P.O. Box 118, S-221 00 Lund, Sweden (diehl@maths.lth.se) (corresponding author), submitted July 4, 2016

reveals as much information on f as possible, is the settling of a suspension in a non-cylindrical vessel (for instance, a cone), as described, under idealizing assumptions, by (1). The solution of this problem of practical interest is, however, involved due to the non-convexity of f in combination with the variability of A. These properties imply that characteristics are not straight lines (in the x-t-plane), and ϕ is not constant along characteristics. In addition, trajectories of admissible concentration discontinuities (shocks) are curved. It is the purpose of this work to explicitly solve the problem (1) for the most relevant case of a function f with one inflection point and a downward-decreasing cross-sectional area A. In particular, we determine the unique entropy solution of (1) in dependence of ϕ_0.

1.2. Related work. Continuous sedimentation is often modelled and simulated in one space dimension [9, 11, 15, 16, 18] since the computational effort for multi-dimensional models is usually excessive. Such one-dimensional models are defined by a nonlinear PDE with spatially discontinuous coefficients because of the inlet and outlets, and may include a strongly degenerate diffusion term describing sediment compressibility [9] in the case of flocculated suspension. All of the cited works presuppose that the function f is known for the suspension under study.

The assumption of one-dimensionality is justified by evidence that in large sedimentation tanks, where the cross-sectional area is constant or decreasing with depth, the concentration profile is essentially one-dimensional [21]. An increasing area, however, easily leads to flows in more dimensions. An example of these two effects is provided in [4]. A downward-contracting cone (sometimes called "Imhoff cone") is widely used for settling tests [6, 24, 29] in wastewater treatment.

In the case of a cylindrical vessel ($A \equiv$ const.) with the model equation $\partial_t \phi - \partial_x f(\phi) = 0$, the identification of $f(\phi)$ has been thoroughly investigated. Treatments based on explicit formulas for discontinuities derived from the PDE include [5, 8, 17, 19] and references cited therein. One limitation with a batch test in a cylindrical vessel is that for low concentrations only the point $(\phi_0, f(\phi_0))$ can be estimated. This is because the constant concentrations on both sides of the liquid-suspension shock wave imply a constant shock speed. In addition to this single point, a part of f can be estimated by tracing the shock after the time point when it becomes curved. When a varying cross-section is used, the concentration below the shock wave varies over an entire interval, yielding a curved shock wave initially. Hence, the flux function can possibly be identified more efficiently. However, an identification method relies on knowledge of the complete solution in each of the possible qualitatively different cases (in dependence on ϕ_0, for given f and A). This motivates the present work.

This work has partly been inspired by the construction of solutions of (1a) with the method of characteristics by Anestis [1] (see also [2]). Anestis treated the case of a concave flux function f, which is a special case of our treatment, which allows f to have one inflection point. The latter is the most common case in modelling sedimentation, but appears also in traffic-flow modelling [31]. Furthermore, numerical solutions of (1), under slightly different assumptions on f, are presented in [7].

As with vehicular traffic flow, pedestrian flow can be modelled with continuum models where the flux is a unimodal function that is zero both for $\phi = 0$ and $\phi = \phi_{\max}$ (the maximum concentration) [32]. The varying $A(x)$ then corresponds to bottlenecks; see [23, 28, 33] and references therein. Equations similar to (1a) model flows in pipes with varying cross-sectional area [13, 26, 30].

1.3. Outline of the paper. In Section 2, we specify the flux functions f and cross-sectional areas A for which we solve the problem (in Section 2.1): only

downward-contracting vessels will be considered; however, many shapes are possible: cones whose silhouette is a straight line, and (not necessarily axisymmetric) vessels with concave or convex silhouettes. Then, in Section 2.2, we define an entropy solution of (1). Section 3 contains preliminaries for the solution of (1): we recall in Section 3.1 the method of characteristics for a general quasilinear first-order PDE from [20], and apply this method in Section 3.2 to obtain an implicit representation of the smooth solution of (1a) (away from discontinuities). In Section 3.3, some geometrical properties of f are recalled. In Section 4, which forms the core of this paper, we construct complete entropy solutions of (1). The part of the solution determined by the initial characteristics from the x-axis is common to all cases and is constant on straight lines in the x-t-plane; see Section 4.1. The entropy solution of (1) is then constructed in each of three qualitatively different cases: Case L, M and H, corresponding to low, middle and high initial concentration ϕ_0 and distinguished by the geometrical properties of $f(\phi)$; see Sections 4.2–4.4. The construction involves new proofs of qualitative properties of curved trajectories of discontinuities that are determined by nonlinear ODEs. These ODEs, and those for the characteristics, are solved numerically for illustration of Cases L, M and H. The results of Section 4 are summarized in Theorem 1 (Section 4.5). Conclusions are collected in Section 5.

2. Problem formulation.

2.1. Assumptions on the flux and area functions. The governing equation in dimensional form is, for time $\tilde{t}$ and height $\tilde{H}$,

$$\partial_{\tilde{t}}\big(\tilde{A}(\tilde{x})\phi\big) - \partial_{\tilde{x}}\big(\tilde{A}(\tilde{x})\tilde{f}(\phi)\big) = 0 \quad \text{for } 0 < \tilde{x} < H \text{ and } \tilde{t} > 0, \tag{2}$$

where H is the height of the suspension and $\tilde{A} \in C^1[0,H]$ is the cross-sectional area. The solid-fluid relative flux function, also called drift flux or Kynch batch flux, $0 \le \tilde{f} \in C^2(0,\phi_{\max})$ is assumed to be unimodal and satisfy $\tilde{f}(0) = \tilde{f}(\phi_{\max}) = 0$. Let $\hat{\phi}$ denote the maximum point of $\tilde{f}$ and $\phi_{\text{infl}} \in (\hat{\phi},\phi_{\max}]$ an inflection point. The flux function can be written as $\tilde{f}(\phi) = \tilde{v}(\phi)\phi$ with $\tilde{v}(\phi) := v_\infty v(\phi)$, where v_∞ is the settling velocity of a single particle and $v(\phi)$ is a dimensionless constitutive function that satisfies $v(\phi_{\max}) = 0$. Hence, $f(\phi) := v(\phi)\phi$ is the dimensionless flux function.

A common semi-empirical flux function is $f(\phi) = \phi(1-\phi)^{r_{\text{RZ}}}$ [27], where $r_{\text{RZ}} \approx 5$ for rigid spheres. This flux function has a zero derivative at $\phi = \phi_{\max} = 1$. To illustrate qualitatively different cases of solutions, we prefer the following flux function:

$$f(\phi) = \phi(\mathrm{e}^{-r_{\text{V}}\phi} - \mathrm{e}^{-r_{\text{V}}\phi_{\max}}) \quad \text{with parameter } r_{\text{V}} > 0 \text{ and } \phi_{\max} = 1. \tag{3}$$

Defining the variables $x := \tilde{x}/H$, $t := \tilde{t}v_\infty/H$, and $A(x) := \tilde{A}(\tilde{x})/\tilde{A}(H)$, we get from (2) the dimensionless hyperbolic PDE (1a). In regions of the x-t-plane where the solution is smooth, (1a) can be written as

$$\partial_t\phi - f'(\phi)\partial_x\phi = \frac{A'(x)}{A(x)}f(\phi). \tag{4}$$

We limit ourselves to the case that A is an invertible function and $A'(x) \ge 0$ for $0 < x < 1$ and that for constants $p, q \ne 0$, the ratio A'/A in (4) can be reduced to

$$\frac{A'(x)}{A(x)} = \frac{1}{p+qx} \quad \Leftrightarrow \quad A(x) = \left(\frac{p+qx}{p+q}\right)^{1/q} \quad \text{for } 0 \leqslant x \leqslant 1. \tag{5}$$

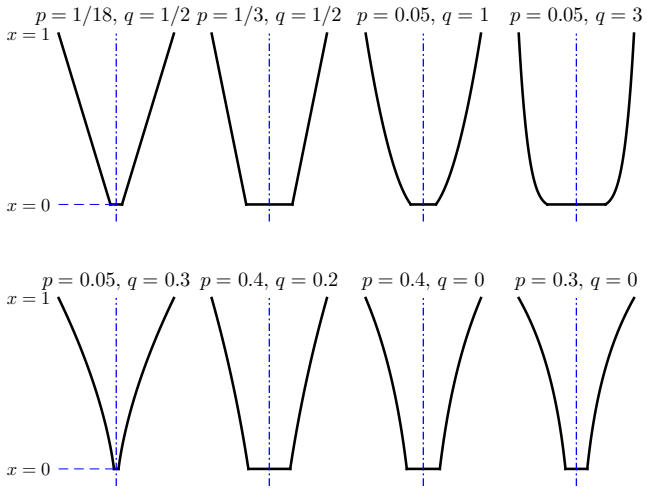

FIG. 1. *Examples of rotational-symmetric vessels with radius function* (7) *with* $m = 2$. *The two first conical vessels are used for the calculated solutions in Figures 2–5. Problem* (1) *is solved for a homogeneous suspension of concentration* ϕ_0 *filled to the top* $x = 1$.

The motivation for this assumption can be found in Section 3.2. Then (4) becomes

$$\partial_t \phi - f'(\phi)\partial_x \phi = \frac{f(\phi)}{p + qx}. \tag{6}$$

The formula (5) implies the following equivalences for $q \neq 0$:

$$\begin{aligned} A(x) > 0,\ A'(x) > 0, \quad 0 \le x \le 1 \quad &\Leftrightarrow \quad p + q > 0,\ p > 0, \quad \text{and} \\ A(x) > 0,\ A'(x) < 0, \quad 0 \le x \le 1 \quad &\Leftrightarrow \quad p + q < 0,\ p < 0. \end{aligned}$$

We consider only $A'(x) > 0$ here. To focus on the main ideas of the proofs below, we avoid $q < 0$ and take $p, q > 0$ as the main case. The special case $q = 0$ gives, instead of (5), the area function $A(x) = \mathrm{e}^{(x-1)/p}$. This is simply the limit case of (5) as $q \to 0^+$, since $(1 + qx/p)^{1/q} \to \mathrm{e}^{x/p}$, a fact that will be utilized in the proofs below.

As for the vessel shape, we may have $\tilde{A}(\tilde{x}) = k\,(\tilde{r}(\tilde{x})/\tilde{r}(H))^m$ for constants $k, m > 0$, and in dimensionless variables,

$$r(x) := \frac{\tilde{r}(\tilde{x})}{\tilde{r}(H)} = \frac{\tilde{r}(xH)}{\tilde{r}(H)}, \qquad A(x) = \frac{\tilde{A}(\tilde{x})}{\tilde{A}(H)} = \left(\frac{\tilde{r}(\tilde{x})}{\tilde{r}(H)}\right)^m = r(x)^m.$$

Hence, with (5) (and $p > 0$, $q > 0$) the "radius" functions we can handle are

$$r(x) = \big((p + qx)/(p + q)\big)^{1/(mq)} \quad \text{for } 0 \leqslant x \leqslant 1. \tag{7}$$

For $mq = 1$, $r(x)$ is affine and in the special case $m = 2 = 1/q$, we get a conical vessel; see Figure 1. This case is used for the computation and illustration of the solutions in Section 4. For the special case $q = 0$, we get $r(x) = A(x)^{1/2} = \mathrm{e}^{(x-1)/(2p)}$.

2.2. Entropy solution. It is well known that solutions of (1a) are smooth in regions of the x-t-plane separated by discontinuities [14]. Discontinuous solutions are not unique in general, and jumps must satisfy an additional condition, the so-called jump entropy condition, to be admissible. These considerations are standard

in conservation law theory (cf., e.g., [20]), and lead to the following concept of entropy solution for (1), where we recall that entropy solutions are unique [25].

DEFINITION 1. *A piecewise smooth function $\phi = \phi(x,t)$ is defined to be an* entropy solution *of (1) if ϕ is continuously differentiable everywhere with the exception of a finite number of curves $x = x_{\rm d}(t) \in C^1$ of discontinuities. At each point $(x_{\rm d}(t)^{\pm}, t)$ of discontinuity, the values $\phi_{\pm} := \phi(x_{\rm d}(t)^{\pm}, t)$ satisfy the jump condition*

$$-x_{\rm d}'(t) = S(\phi_+,\phi_-) := \begin{cases} \big(f(\phi_+) - f(\phi_-)\big)/(\phi_+ - \phi_-) & \text{if } \phi_+ \neq \phi_-, \\ f'(\phi) & \text{if } \phi_+ = \phi_- =: \phi, \end{cases} \tag{8}$$

and the jump entropy condition

$$S(u,\phi_-) \geq S(\phi_+,\phi_-) \quad \text{for all } u \text{ between } \phi_+ \text{ and } \phi_-. \tag{9}$$

It is well known that entropy solutions in the sense of Definition 1 are also the unique entropy solutions in the sense of Kružkov-type integral inequalities (cf., e.g., [20]). That formulation is usually employed to demonstrate convergence of finite volume schemes [9, 10, 20] to an entropy solution. Consequently, such a numerical scheme (e.g., of monotone type) applied to (1) approximates the exact solutions constructed herein (in dependence of ϕ_0) (see Figure 4 (b) below). The constructed solutions here can therefore be employed to measure the performance of numerical schemes.

3. Preliminaries.

3.1. Characteristics for a quasilinear, first-order PDE. Suppose we wish to solve the following non-homogeneous, quasi-linear first-order PDE for $u = u(x,t)$:

$$a(x,t,u)\partial_t u + b(x,t,u)\partial_x u = c(x,t,u), \quad (x,t) \in \Omega \subset \mathbb{R}^2 \tag{10}$$

and assume that $\Gamma \subset \mathbb{R}^3$ is a curve parametrized by $\nu \mapsto (x(\nu), t(\nu), z(\nu))$ that represents given data, for example initial data when t is constant. In other words we seek a surface $S = \{(x,t,u(x,t))|(x,t) \in \Omega\} \subset \mathbb{R}^3$ such that $\Gamma \subset S$ and $u(x,t)$ is a solution of (10). To this end, one solves the following system of first-order ODEs for $\eta \geqslant \eta_0$, where a, b and c are evaluated at $(x(\nu,\eta), t(\nu,\eta), z(\nu,\eta))$:

$$\partial_\eta t = a,\ t(\nu,\eta_0) = t(\nu); \quad \partial_\eta x = b,\ x(\nu,\eta_0) = x(\nu); \quad \partial_\eta z = c,\ z(\nu,\eta_0) = z(\nu). \tag{11}$$

Suppose that we may invert the relations $x = x(\nu,\eta)$ and $t = t(\nu,\eta)$ to give $\nu = \nu(x,t)$ and $\eta = \eta(x,t)$. One can then show that $u = z(\nu(x,t),\eta(x,t))$ indeed is a solution of (10) and that $\Gamma \subset S$. The equations (11) are the so-called *characteristic equations*, and their solutions are the *characteristics* of (10).

3.2. Smooth solutions away from discontinuities. Consider equation (4) with the only restriction $A' > 0$. Since the coefficient for $\partial_t\phi$ is 1, the characteristic curves (or characteristics) associated with (4) can be parametrized by time t. Assume that the characteristics emanate from a piece of curve in x-t-ϕ-space with initial data $(x,t,\phi) = (\xi,\tau,\varphi)$, where ξ, τ and φ are scalar parameterized functions each taking values in a closed bounded interval. This can be the initial piece of line $(x,t,\phi) = (\xi,0,\phi_0)$, where $\xi \in (0,1)$ is the parameter and ϕ_0 is constant, or a part of a contact discontinuity from which characteristics emanate tangentially (τ is a natural parameter). Along each characteristic curve (in the x-t-ϕ-space), the variations of the

spatial coordinate and the volume fraction are given by the solutions $x = X(t)$ and $\phi = \Phi(t)$ of the following ODEs for $t \geq \tau$ (the characteristic equations in this case):

$$X'(t) = -f'(\Phi), \qquad \Phi'(t) = A'(X)f(\Phi)/A(X), \tag{12}$$

along with the initial data $(X(\tau), \Phi(\tau)) = (\xi, \varphi)$. These equations immediately provide the following information for $0 < \Phi < \phi_{\max}$. Since $A' > 0$, the volume fraction $\Phi(t)$ increases along each characteristic. For convenience, the projection of the characteristics onto the x-t-plane are also called "characteristics". If $\Phi(0) = \varphi < \hat{\phi}$, then $X'(t) = -f'(\Phi) < 0$ for small $t > 0$, which means that the characteristics are initially directed downwards. As Φ increases and passes $\Phi = \hat{\phi}$ along a characteristic, the characteristic turns upward; cf. Figure 2. Furthermore, characteristics are (geometrically) convex for $\Phi < \phi_{\mathrm{infl}}$ and concave for $\Phi > \phi_{\mathrm{infl}}$, since

$$X''(t) = -f''(\Phi)\Phi'(t). \tag{13}$$

Equations (12) yield $\mathrm{d}\log f(\Phi)/\mathrm{d}y = -\mathrm{d}\log A(X)/\mathrm{d}t$, which we can integrate along a characteristic from $t = \tau$ to a later time point $t > \tau$:

$$\log \frac{f(\phi)}{f(\varphi)} = -\log \frac{A(x)}{A(\xi)} \quad \Leftrightarrow \quad \frac{f(\phi)}{f(\varphi)} = \frac{A(\xi)}{A(x)}. \tag{14}$$

Since A is an invertible function, we can solve this equality for x as a function of the other variables: $x = \bar{A}(\phi, \xi, \varphi)$. Then we can express the right-hand side of the second equation of (12) as a function of Φ and the initial values:

$$\Phi'(t) = A'\big(\bar{A}(\Phi, \xi, \varphi)\big) f(\Phi)^2 / \big(A(\xi) f(\varphi)\big)$$

Rearranging and integrating from $t = \tau$ to a later time point t, we get together with (14) the following system of equations:

$$t - \tau = A(x)f(\phi) \int_{\varphi}^{\phi} \frac{\mathrm{d}\Phi}{A'(\bar{A}(\Phi, \xi, \varphi)) f(\Phi)^2}, \qquad \frac{f(\phi)}{f(\varphi)} = \frac{A(\xi)}{A(x)}. \tag{15}$$

For the given one-parameter curve of initial values (ξ, τ, φ), system (15) defines ϕ as a function of x and t. Since (ξ, τ, φ) depends on one parameter, this can in principle be achieved by solving the second equation for one variable and substituting the result into the first, so that a single equation implicitly defines $\phi = \phi(x, t)$ as long as the characteristics do not intersect each other or a discontinuity.

The presence of A' in the integrand of (15) complicates the analysis. By a similar derivation as above, area functions of the form (5) lead to the simpler system

$$t - \tau = (p + qx) f(\phi)^q \int_{\varphi}^{\phi} \frac{\mathrm{d}\Phi}{f(\Phi)^{1+q}}, \qquad \frac{f(\phi)}{f(\varphi)} = \left(\frac{p + q\xi}{p + qx} \right)^{1/q}. \tag{16}$$

The special case $A(x) = \mathrm{e}^{(x-1)/p}$ is obtained as $q \to 0^+$; for example, the right equation becomes $f(\phi)/f(\varphi) = \mathrm{e}^{(\xi - x)/p}$.

3.3. Geometric properties of a flux function with one inflection point.

LEMMA 2. *The function $v(\phi) = f(\phi)/\phi$ satisfies $v'(\phi) < 0$ for $0 < \phi < \phi_{\max}$.*

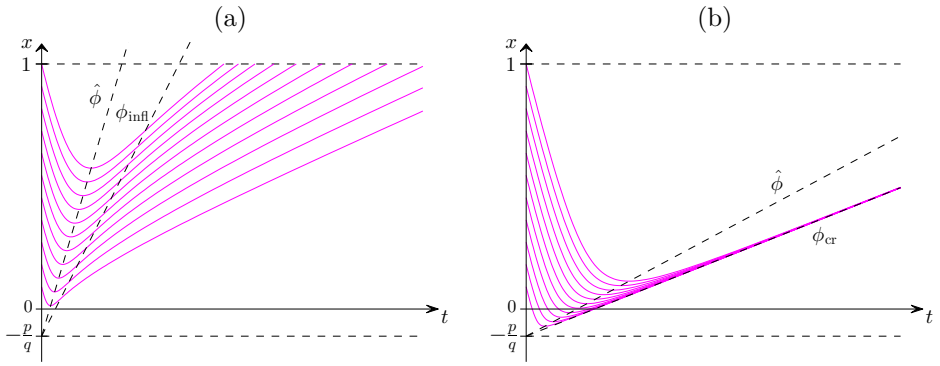

FIG. 2. *Illustration of Lemma 4 with characteristics, whose paths are calculated from* $0 < x < 1$, $t = 0$. *The flux function and cross-sectional are are described by* $r_{\text{V}} = 4$, $p = 1/18$, $q = 1/2$. (a) *The case* $\phi_0 = 0.04$ *results in* $Q'(\phi) > 0$ *for* $0 < \phi < \phi_{\max}$, *so that the characteristics do not intersect. The dashed lines are given by* (21) *with the concentrations* $\hat{\phi} = 0.238$ *and* $\phi_{\text{infl}} = 2/r_{\text{V}} = 0.5$. (b) *The case with* $\phi_0 = 0.001$ *results in conglomerating characteristics at the concentration* $\phi_{\text{cr}} = 0.32 < \phi_{\text{infl}} = 0.5$. *All characteristics approach the corresponding straight line* (21) *with* $\phi = \phi_{\text{cr}}$.

Proof. We have $v'(\phi) = g(\phi)/\phi^2$ with $g(\phi) := f'(\phi)\phi - f(\phi)$. Now, $g(0) = 0$ and $g'(\phi) = f''(\phi)\phi < 0$ for $0 < \phi < \phi_{\text{infl}}$; hence $g(\phi) < 0$ for $0 < \phi \leq \phi_{\text{infl}}$. Thus, $v'(\phi) < 0$ for $0 < \phi \leqslant \phi_{\text{infl}}$. For any fixed $\phi \in (\phi_{\text{infl}}, \phi_{\max})$, the mean-value theorem gives that there exists a $\xi \in (\phi, \phi_{\max})$ such that $f'(\phi) = f'(\phi_{\max}) + f''(\xi)(\phi - \phi_{\max}) < 0$. Hence, $g(\phi) < 0$ and also $v'(\phi) < 0$ for $\phi_{\text{infl}} < \phi < \phi_{\max}$. ∎

In the construction of solutions, more precisely in the vicinity of discontinuities, we need the following operations introduced by Ballou [3]; see also [12]. We define

$$\phi^* := \sup\big\{u > \phi : S(\phi, u) \leq S(\phi, v)\ \forall v \in (\phi, u]\big\} \quad \text{for } \phi \in [0, \phi_{\text{infl}}], \tag{17}$$

$$\phi^{**} := \inf\big\{u < \phi : u^* = \phi\big\} \quad \text{for } \phi \in [\phi_{\text{infl}}, \phi_{\max}]. \tag{18}$$

We collect some properties of the operation * in the following lemma [3].

LEMMA 3. *The function* $\phi^* = \phi^*(\phi) \in C^1$ *satisfies the following:*
(i) *For given* $\phi < \phi_{\text{infl}}$, ϕ^* *is the unique solution of* $S(\phi, u) = f'(u)$, $u > \phi_{\text{infl}}$.
(ii) $f'(\phi) > S(\phi, \phi^*) = f'(\phi^*)$.
(iii) $\mathrm{d}\phi^*/\mathrm{d}\phi < 0$.

By property (iii), the operation * is invertible and the inverse operation is ** given by (18). If the flux function satisfies $f'(\phi_{\max}) < 0$, then $\phi^* > \phi_{\max}$ for $\phi \in [0, \phi^{**}_{\max})$.

4. Construction of the entropy solution. We construct the entropy solution of (1) when $A(x)$ is given by (5) and state the theorem at the end of this section.

4.1. Solution defined by characteristics from $t = 0$. Consider the initial curve $(x, t, \phi) = (\xi, 0, \phi_0)$, where $\xi \in (0, 1)$ is the parameter and ϕ_0 is a constant. Then solely the first equation of (16) defines the solution $\phi = \phi(x, t)$ implicitly:

$$\psi(x, t) = Q(\phi), \qquad \text{where} \tag{19}$$

$$\psi(x, t) := t/(p + qx) \quad \text{and} \quad Q(\phi) := f(\phi)^q \int_{\phi_0}^{\phi} \frac{\mathrm{d}\Phi}{f(\Phi)^{1+q}}, \quad \phi \in [\phi_0, \phi_{\max}). \tag{20}$$

This includes the special case $q = 0$. For $q > 0$, (22) can be written as

$$x = t/(qQ(\phi)) - p/q; \tag{21}$$

hence, ϕ is constant on straight lines in the x-t-plane which all intersect the x-axis at $x = -p/q < 0$; see Figure 2 and the following lemma.

LEMMA 4. *Assume that $p, q > 0$ and that the initial datum $\phi(x,0) = \phi_0$ for (6) is given on the half line $x > -p/q$. If $Q'(\phi) > 0$ for $\phi_0 \leq \phi < \phi_{\max}$, then the solution*

$$\phi(x,t) = Q^{-1}\big(\psi(x,t)\big), \tag{22}$$

is smooth and defined along all its characteristics (in the x-t-plane), which never intersect. Then define $\phi_{\mathrm{cr}} := \phi_{\max}$. Otherwise there exists a unique zero $\phi_{\mathrm{cr}} \in (\hat{\phi}, \phi_{\mathrm{infl}}]$ of Q' (the volume fraction of conglomerating characteristics) such that $Q'(\phi) > 0$ for $\phi \in [\phi_0, \phi_{\mathrm{cr}})$ and (22) is defined, satisfies $\phi(x,t) < \phi_{\mathrm{cr}}$ and is smooth in the region

$$x > t/(qQ(\phi_{\mathrm{cr}})) - p/q, \qquad t > 0. \tag{23}$$

In both cases, the solution satisfies $\partial_t \phi > 0$ and $\partial_x \phi < 0$.

Proof. We prove that the smooth function Q is invertible. We have $Q(\phi_0) = 0$ and

$$Q'(\phi) = f'(\phi) q f(\phi)^{q-1} \int_{\phi_0}^{\phi} \frac{\mathrm{d}\Phi}{f(\Phi)^{1+q}} + \frac{1}{f(\phi)} = q f(\phi)^{q-1} P(\phi), \quad \text{where} \tag{24}$$

$$P(\phi) := f'(\phi) \int_{\phi_0}^{\phi} \frac{\mathrm{d}\Phi}{f(\Phi)^{1+q}} + \frac{1}{q f(\phi)^q}, \quad \phi \in [\phi_0, \phi_{\max}). \tag{25}$$

We have $Q'(\phi) > 0$ at least for $\phi \in [\phi_0, \hat{\phi}]$, since $f'(\phi) \geqslant 0$ in that interval. Since $f \in C^2$, the function P belongs to C^1. It satisfies $P(\phi_0) > 0$ and its derivative is

$$P'(\phi) = f''(\phi) \int_{\phi_0}^{\phi} \frac{\mathrm{d}\Phi}{f(\Phi)^{1+q}} \begin{cases} < 0 & \text{for } \phi_0 < \phi < \phi_{\mathrm{infl}}, \\ = 0 & \text{for } \phi = \phi_{\mathrm{infl}}, \\ > 0 & \text{for } \phi_{\mathrm{infl}} < \phi < \phi_{\max}, \end{cases} \tag{26}$$

i.e., P has a unique minimum at ϕ_{infl}. If $P(\phi_{\mathrm{infl}}) > 0$, then $Q'(\phi) > 0$ for all $\phi \in [\phi_0, \phi_{\max}]$ and Q is invertible on its whole domain (the characteristics do not intersect). If $P(\phi_{\mathrm{infl}}) \leqslant 0$, then there exists a (unique) zero $\phi_{\mathrm{cr}} \in (\hat{\phi}, \phi_{\mathrm{infl}}]$ of P and hence of Q'. Since ϕ increases along the characteristics, (19) defines a smooth function as long as $\phi(x,t) < \phi_{\mathrm{cr}}$. Then $\partial_t \phi = \partial_t \psi / Q'(\phi) < 0$ and $\partial_x \phi = \partial_x \psi / Q'(\phi) > 0$ since

$$\partial_x \psi = -qt/(p+qx)^2 < 0, \qquad \partial_t \psi = 1/(p+qx) > 0. \tag{27}$$

∎

LEMMA 5. *Consider problem (6) with initial datum $\phi(x,0) = \phi_0$ for $x \in \mathbb{R}$ in the case $p > 0$, $q = 0$, i.e. for $A(x) = \mathrm{e}^{(x-1)/p}$. Then the solution is given by*

$$\phi(x,t) = Q^{-1}\big(t/p\big), \quad t > 0, \tag{28}$$

and it satisfies $\partial_t \phi > 0$ and $\partial_x \phi = 0$.

Proof. When $q = 0$, (19) is equivalent to (28) if Q^{-1} exists, which is the case for $\phi \in [\phi_0, \phi_{\max})$, since there $Q'(\phi) = 1/f(\phi) > 0$. ∎

For completeness, we define $\phi_{\mathrm{cr}} := \phi_{\max}$ also in the case $q = 0$.

4.2. Case L: $\phi_0 \leqslant \phi_{\max}^{**}$. Figure 3 shows the solution, in which the bottom discontinuity may or may not reach the upper shock wave (sediment level). The case $0 < \phi_0 \leqslant \phi_{\max}^{**}$ is shown, which implies that $f'(\phi_{\max}) < 0$, because $f'(\phi_{\max}) = 0$ implies $\phi_{\max}^{**} = 0$. Figure 4 (a) provides an enlarged view of parts of the solution near the origin, and Figure 4 (b) displays a numerical solution of the scenario of Figure 3 (e) computed with an entropy-satisfying finite volume scheme (see e.g. [7, 16]).

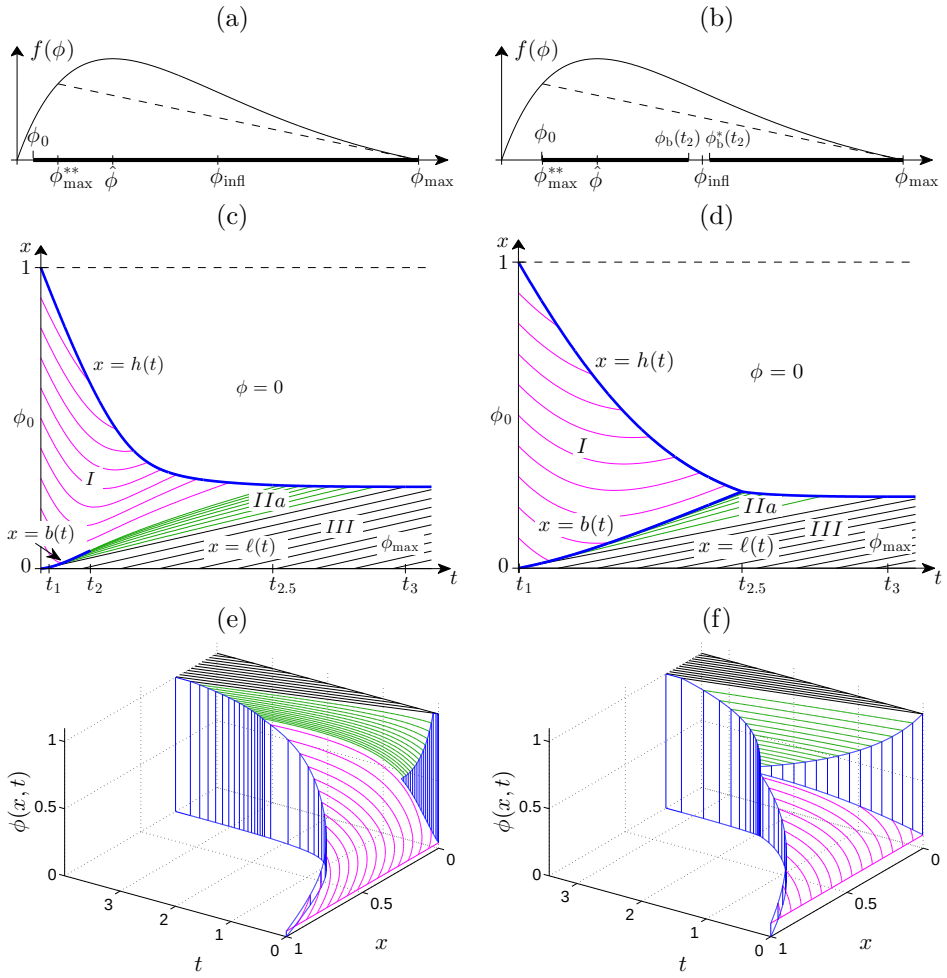

FIG. 3. *Case L:* $\phi_0 \leqslant \phi^{**}_{\max}$*, where* (a, c, e) $\phi_0 = 0.04$ *and* $p = 1/18$*, and* (b, d, f) $\phi_0 = 0.1$ *and* $p = 1/3$*, implying non-intersection and intersection of the two discontinuities, respectively, shown by thick blue curves.* (a, b) *Graphs of the flux function* (3) *in both cases with* $r_{\text{V}} = 4$*,* $\phi^{**}_{\max} = 0.102$*,* $\hat\phi = 0.238$*,* $\phi_{\text{infl}} = 0.5$ *and* $\phi_{\max} = 1$*. The thick interval on the respective* ϕ*-axis shows the concentrations appearing in the solution just below the sediment level.* (c–f)*: Characteristics in 2D and 3D shown by thin curves (except for the vertical blue lines below the discontinuities in the 3D plot). In* (c, e)*, the bottom contact discontinuity ends at time* $t_2 = 0.501$ *since the concentration values on both sides equal* ϕ_{infl}*. In* (d, f)*, the two discontinuities intersect at* $t_2 = t_{2.5} = 1.931$*.*

Case L: The upper boundary of region I. Between the clear liquid and the suspension, there is a discontinuity (sediment level) whose location we denote by $x = h(t)$. This starts at the point $(x, t) = (1, 0)$ and satisfies the jump condition (8):

$$-h'(t) = S\big(\phi_h(t), 0\big) = \frac{f(\phi_h(t))}{\phi_h(t)} = v(\phi_h(t)), \tag{29}$$

where $\phi_h(t) := \phi(h(t)^-, t)$ is the volume fraction just below the interface. We have $\phi_h(0) = \phi_0 \in (0, \phi^{**}_{\max}]$ and as long as $\phi_h(t) < \phi_{\max}$, there holds $h'(t) < 0$ so the shock is directed downward. For $\phi_h(t) = \phi_{\max}$, we have $h'(t) = v(\phi_{\max}) = 0$. Thus, the boundary condition (1c) at $x = 1$ is satisfied. The discontinuity satisfies (9), since by

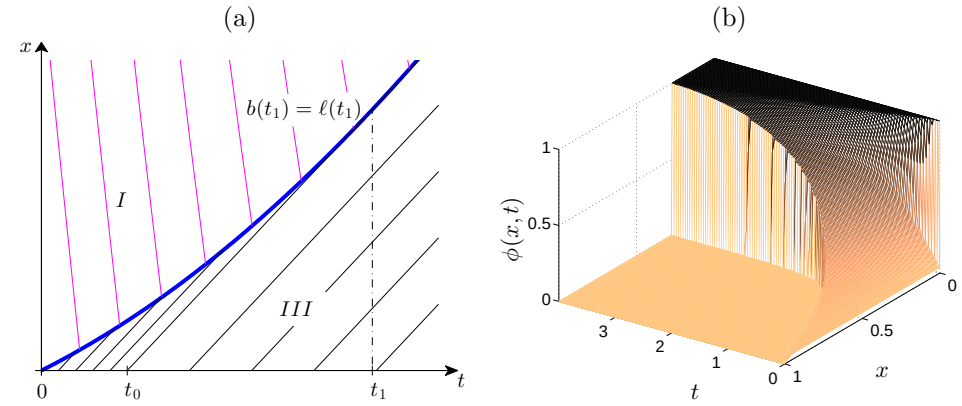

FIG. 4. (a) *Enlarged view near the origin of Figure 3 (c). The curves $x = b(t)$ and $x = \ell(t)$ intersect at $t_1 = 0.0845$. The time point $t_0 = 0.0218$ is the intersection of $x = \ell(t)$ with the t-axis.* (b) *Numerical solution of the scenario computed with an entropy-satisfying scheme [7, 16]. Results agree completely with the constructed solution of Figure 3 (e).*

Lemma 2

$$S(u,0) = \frac{f(u)}{u} = v(u) > v\big(\phi_h(t)\big) = \frac{f(\phi_h(t))}{\phi_h(t)} = S\big(\phi_h(t),0\big) \quad \forall u \in (0,\phi_h(t)). \tag{30}$$

The discontinuity is a shock wave, since characteristics on both sides enter it with positive angles when followed in the direction of increasing t. This can be seen from (12) and Lemma 2 in the following way. The characteristics above the shock satisfy

$$X'(t) = -f'(0) = -\big(v'(0)\cdot 0 + v(0)\big) = -v(0) < -v(\phi_h(t)) = h'(t).$$

and under the assumption that the solution below the shock satisfies $\phi_h(t) > 0$ for $t \geq 0$ (which will be proved in the next lemma), we have

$$X'(t) = -f'(\phi_h(t)) = -\left[v'(\phi_h(t))\phi_h(t) + v(\phi_h(t))\right] > -v(\phi_h(t)) = h'(t).$$

LEMMA 6. *The discontinuity $x = h(t)$, $0 \leq t < T$, is a shock wave satisfying the jump and entropy conditions (8) and (9), $h(0) = 1$, $h'(t) < 0$ and $h''(t) > 0$. The solution ϕ of (1a) is zero for $x > h(t)$ and just below the shock the solution values are given by the increasing function*

$$\phi_h(t) = Q^{-1}\big(\psi(h(t),t)\big), \tag{31}$$

where ψ is defined in (20). The time T is the supremum of the time points when $\phi_h(t)$ is defined by values along characteristics from $t = 0$ having values less than ϕ_{cr}.

Proof. Some of the statements were proved before the lemma. Differentiating (31) and utilizing the identity $(Q^{-1})'(Q(\phi)) = 1/Q'(\phi) > 0$, we get

$$\phi_h'(t) = \frac{\partial_x\psi(h(t),t)h'(t) + \partial_t\psi(h(t),t)}{Q'(\phi_h(t))} > 0, \tag{32}$$

since $Q' > 0$ by Lemma 4, $h' < 0$ by (29), and (27). (In the special case $q = 0$, the same conclusion is drawn with $\psi(x,t) = t/p$.) Substituting (31) into (29) we

get the ODE $-h'(t) = v(Q^{-1}(\psi(h(t),t)))$, $h(0) = 1$, for the location of the upper discontinuity. The right-hand side of this ODE is a Lipschitz continuous function as long as $x = h(t)$ satisfies (23) and hence gives a unique solution. Since $v' < 0$ by Lemma 2 and $\phi_h'(t) > 0$ by (32), we get $-h''(t) = v'(\phi_h(t))\phi_h'(t) < 0$. ∎

Case L: The lower boundary of region I. At $(x,t) = (0,0)$, a discontinuity is created between ϕ_0 and $\phi_{\max}$ and we denote its location by $x = b(t)$.

LEMMA 7. *The bottom discontinuity $x = b(t)$, $0 \le t < t_2$, satisfies the jump and entropy conditions (8) and (9), $b(0) = 0$, $b'(t) > 0$ and $b''(t) > 0$. The characteristics above the discontinuity $x = b(t)$ enter it with positive angles. The solution values just above $x = b(t)$ are given by the increasing function*

$$\phi_b(t) := \phi\big(b(t)^+, t\big)\big) = Q^{-1}\big(\psi(b(t),t)\big) \tag{33}$$

that satisfies $\phi_b(0) = \phi_0 < \phi^{**}_{\max}$. Either $b(t)$ meets the upper discontinuity at $t = t_2$, i.e., $b(t_2) = h(t_2)$, or it satisfies $\phi_b(t_2) = \phi_{\text{infl}} = \phi_b^*(t_2) = \phi_b(t_2^+)$, i.e., it ceases to exist at time t_2. The solution in $0 < x < b(t)$ is $\phi(x,t) = \phi_{\max}$ for $0 \le t < t_1$, where t_1 is defined by $\phi_b(t_1) = \phi^{**}_{\max}$ (assuming $t_1 \le t_2$; otherwise set $t_1 := t_2$). There exists a constant ϕ_G such that $\phi_b(t) < \phi_G < \phi_{\text{cr}}$, $0 \le t < t_2$. The discontinuity $x = b(t)$ is a shock wave for $0 \le t < t_1$ and a contact discontinuity for $t_1 < t < t_2$.

Proof. The jump condition (8) is

$$-b'(t) = S\big(\phi_b(t), \phi_b^-(t)\big), \tag{34}$$

where the volume fraction $\phi_b(t)$ just above the discontinuity is (33) according to Lemma 4, and the corresponding value $\phi_b^-(t)$ just below is given by

$$\phi_b^-(t) := \phi\big(b(t)^-, t\big)\big) = \begin{cases} \phi_{\max} & \text{for } 0 \leqslant \phi_b(t) \leqslant \phi^{**}_{\max}, \\ \phi_b^*(t) & \text{for } \phi^{**}_{\max} \leqslant \phi_b(t) \leqslant \phi_{\text{infl}}. \end{cases}$$

It can be seen from (17) and (18) that the entropy condition (9) is satisfied. Furthermore, $b'(t) > 0$, i.e., the discontinuity is directed upward, since

$$\begin{aligned} -b'(t) &= S\big(\phi_b(t), \phi_b^-(t)\big) \\ &= \begin{cases} S\big(\phi_b(t), \phi_{\max}\big) = \dfrac{f(\phi_b(t))}{\phi_b(t) - \phi_{\max}} & \text{for } 0 \leqslant \phi_b(t) \leqslant \phi^{**}_{\max}, \\ S\big(\phi_b(t), \phi_b^*(t)\big) = f'(\phi_b^*(t)) & \text{for } \phi^{**}_{\max} \leqslant \phi_b(t) \leqslant \phi_{\text{infl}}. \end{cases} \end{aligned} \tag{35}$$

By inserting (33) into (34) an ODE is obtained with the initial value $b(0) = 0$. As long as $\phi_b(t) < C < \phi_{\text{cr}}$ for some constant C (which by Lemma 4 is equivalent to $x = b(t)$ satisfying (23) with margin), Lemma 3 and (24) imply that the right-hand side of (34) is C^1 and Lipschitz continuous, so that $b(t)$ is the unique smooth solution satisfying $b(0) = 0$. Inserting this into (33) we get the values of the smooth function $\phi_b(t)$. We know that $\phi_b(0) = \phi_0 < \phi^{**}_{\max}$. Thus $0 < \phi_b(t) < \phi^{**}_{\max}$ for small times, hence the characteristics above enter the discontinuity under positive angles, since

$$X'(t) = -f'(\phi_b(t)) < 0 < -\frac{f(\phi_b(t))}{\phi_b(t) - \phi_{\max}} = -S\big(\phi_b(t), \phi_b^-(t)\big) = b'(t).$$

For $\phi^{**}_{\max} \leqslant \phi_b(t) \leqslant \phi_{\text{infl}}$, Lemma 3 (i) implies $X'(t) = -f'(\phi_b(t)) < -f'(\phi_b^*(t))$. We shall now prove that b is convex and that $\phi_b(t) < \phi_G < \phi_{\text{cr}}$ for some constant ϕ_G.

The case $q = 0$ is simple, since then $\phi_b'(t) = f(\phi_b(t))/p > 0$. Assume that $q > 0$. Differentiating (33) and utilizing (21) and (34), we get

$$\phi_b'(t) = \frac{\psi_x(b(t),t)b'(t) + \psi_t(b(t),t)}{Q'(\phi_b(t))} = \frac{1}{Q'(\phi_b(t))}\left(\frac{qtS(\phi_b(t),\phi_b^-(t))}{(p+qb(t))^2} + \frac{1}{p+qb(t)}\right)$$

$$= \frac{qt}{Q'(\phi_b(t))(p+qb(t))^2}\left(S\big(\phi_b(t),\phi_b^-(t)\big) + \frac{1}{Q(\phi_b(t))}\right). \tag{36}$$

The first factor is positive for $t > 0$. To see that the second factor is also positive, we define the continuous function $G(\phi_b) := S(\phi_b,\phi_b^-) + 1/Q(\phi_b)$ for $\phi_b > \phi_0$, where $S(\phi_b,\phi_b^-)$ is given by (35). Both terms of G are decreasing continuous functions of ϕ_b, partly by (24) and partly by $\mathrm{d}\phi^*/\mathrm{d}\phi < 0$ (see Lemma 3), since

$$\frac{\mathrm{d}}{\mathrm{d}\phi_b}S(\phi_b,\phi_b^-) = \begin{cases} \dfrac{f'(\phi_b)(\phi_b-\phi_{\max}) - f(\phi_b)}{(\phi_b-\phi_{\max})^2} < 0 & \text{for } 0 \leqslant \phi_b \leqslant \phi_{\max}^{**}, \\ f''(\phi_b^*)\mathrm{d}\phi_b^*/\mathrm{d}\phi_b < 0 & \text{for } \phi_{\max}^{**} \leqslant \phi_b \leqslant \phi_{\mathrm{infl}}. \end{cases} \tag{37}$$

Note that the upper row of (37) is obvious if $f'(\phi_{\max}^{**}) \geq 0$. In the case $f'(\phi_{\max}^{**}) < 0$, i.e. $\hat\phi < \phi_{\max}^{**} < \phi_{\mathrm{infl}}$, then the inequality can be established by the properties of f and the mean-value theorem (we skip the details). We also have

$$\lim_{\phi_b\to\phi_0^+} G(\phi_b) = \lim_{\phi_b\to\phi_0^+}\frac{1}{Q(\phi_b)} = \infty.$$

We recall that ϕ_{cr} is the zero of P (see (25)), so by the definition of Q (20) we get

$$Q(\phi_{\mathrm{cr}}) := f(\phi_{\mathrm{cr}})^q\int_{\phi_0}^{\phi_{\mathrm{cr}}}\frac{\mathrm{d}\Phi}{f(\Phi)^{1+q}} = \frac{f(\phi_{\mathrm{cr}})^q}{f'(\phi_{\mathrm{cr}})}\left(P(\phi_{\mathrm{cr}}) - \frac{1}{qf(\phi_{\mathrm{cr}})^q}\right) = -\frac{1}{qf'(\phi_{\mathrm{cr}})}.$$

This can be used to conclude that

$$G(\phi_{\mathrm{cr}}) = \begin{cases} \dfrac{f(\phi_{\mathrm{cr}})}{\phi_{\mathrm{cr}}-\phi_{\max}} - qf'(\phi_{\mathrm{cr}}) < 0 & \text{if } 0 \leqslant \phi_{\mathrm{cr}} \leqslant \phi_{\max}^{**}, \\ f'(\phi_{\mathrm{cr}}^*) - qf'(\phi_{\mathrm{cr}}) < 0, & \text{if } \phi_{\max}^{**} \leqslant \phi_{\mathrm{cr}} \leqslant \phi_{\mathrm{infl}}, \end{cases}$$

where the latter inequality follows from Lemma 3 (i). Hence, G has a unique zero $\phi_G \in (\phi_0,\phi_{\mathrm{cr}})$, so $\phi_b(t) \equiv \phi_G$ is an orbit of the ODE (36). The solution orbit we are interested cannot cross this (since for any constants C_1, C_2 satisfying $\phi_0 < C_1 < C_2 < \phi_{\mathrm{cr}}$ the right-hand side of (36) is a Lipschitz continuous function of ϕ_b for $\phi_0 < C_1 \leqslant \phi_b \leqslant C_2 < \phi_{\mathrm{cr}}$) and satisfies therefore $\phi_0 = \phi_b(0) < \phi_b(t) < \phi_G$ and $\phi_b'(t) > 0$ for $t > 0$ until the bottom discontinuity meets the upper one, which occurs at some finite time point t_2 since $h'(t) < 0$ according to Lemma 6. Next we differentiate (34) and use (37) to see that

$$-b''(t) = \frac{\mathrm{d}}{\mathrm{d}t}S\big(\phi_b(t),\phi_b^-(t)\big) = \frac{\mathrm{d}S}{\mathrm{d}\phi_b}\big(\phi_b(t),\phi_b^-(t)\big)\phi_b'(t) < 0.$$

Now that we know that $\phi_b(t)$ is increasing and $\phi_b(0) = \phi_0 < \phi_{\max}^{**}$, let $t_1 > 0$ be the time when $\phi_b(t_1) = \phi_{\max}^{**}$. If the upper and lower discontinuities meet before t_1 then set $t_1 := t_2$. In any case, $\phi_b(t) = \phi_{\max}$ for $t \in [0,t_1)$ and the characteristics in $0 < x < b(t)$ all have the slope $\mathrm{d}X/\mathrm{d}t = -f'(\phi_{\max}) > 0$. Furthermore, they go into the bottom discontinuity from below with positive angle (hence it is a shock), since

$$X'(t) = -f'(\phi_{\max}) > -S\big(\phi_b(t),\phi_{\max}\big) = -S\big(\phi_b(t),\phi_b^-(t)\big) = b'(t), \quad 0 \leqslant t < t_1.$$

The characteristic and the bottom discontinuity are tangential at $t = t_1$ since

$$X'(t_1) = -f'(\phi_{\max}) = -S\big(\phi^{**}_{\max}, \phi_{\max}\big) = -S\big(\phi_b(t_1), \phi_b^-(t_1)\big) = b'(t_1). \tag{38}$$

Assume that $t_2 > t_1$. The fact that we have defined $\phi_b^+(t) = \phi_b^*(t)$ when $\phi_b(t) \geq \phi^{**}_{\max}$, which occurs for $t \geq t_1$, gives for the characteristics below the discontinuity:

$$X'(t) = -f\big(\phi_b^*(t)\big) = -S\big(\phi_b(t), \phi_b^*(t)\big) = -S\big(\phi_b(t), \phi_b^-(t)\big) = b'(t).$$

Hence, the characteristics emanate tangentially from the contact discontinuity $x = b(t)$, $t_1 \leqslant t \leqslant t_2$. ∎

Lemma 7 yields the following. Either the bottom and upper shock waves intersect and $\phi_b(t) < \phi_G < \phi_{\rm cr}$, $0 \leq t \leq t_2$, which is equivalent to the fact that $x = b(t)$ always satisfies (23), i.e. the bottom discontinuity never reaches the line of conglomerating characteristics. Otherwise the shock $x = b(t)$ disappears at $x = b(t_2) < h(t_2)$ since the concentrations on both sides tend to $\phi_{\rm infl}$. Then the rest of the boundary of region I is defined by the characteristic that starts from $t = 0$ and passes $(x, t) = (b(t_2), t_2)$. Since $\Phi(t_2) = \phi_{\rm infl}$ and the concentration $\Phi(t)$ increases, the characteristic is concave for $t_2 \leq t \leq t_{2.5}$, where $t_{2.5}$ is the time point it meets the upper shock wave. In the former case when $x = b(t)$ and $x = h(t)$ intersect, we defined $t_{2.5} := t_2$.

Case L: The solution in regions IIa and III. The time points t_1, t_2 and $t_{2.5}$ are defined above. If $t_1 = t_2$, then the upper and lower discontinuities of region I intersect before $\phi_b(t)$ has increased to $\phi^{**}_{\max}$. By the construction in this subsection the entire solution in this case has $t_1 = t_2 = t_{2.5} = t_3$, so that region IIa is empty.

We now assume that $t_1 < t_2 \leq t_{2.5}$. Then $\phi_b(t_1) = \phi^{**}_{\max}$, and the characteristic going into the shock wave from below to the point $(x, t) = (b(t_1), t_1)$ has the equation

$$x = \ell(t) := -f'(\phi_{\max})(t - t_1) + b(t_1). \tag{39}$$

This characteristic carries $\phi = \phi_{\max} = (\phi^{**}_{\max})^*$ and is tangential to $x = b(t)$ at $t = t_1$ because of (38). Since $x = b(t)$ is convex, (39) is the valid equation for a characteristic also for $t_1 < t < t_3$, where $t_3 > t_{2.5}$ is the time point when this line meets the upper discontinuity $x = h(t)$ (to be defined for $t > t_{2.5}$). We let (39) define the boundary between regions IIa and III for $t_1 \leq t \leq t_3$. Clearly, $x = h(t)$ for $t \geq t_3$ is an entropy-satisfying shock with constant speed separating 0 and $\phi_{\max}$.

LEMMA 8. *For $0 \leq t \leq t_3$ and $t \neq t_1$, (39) is a line along which the solution is continuous. In region III, the solution is $\phi_{\max}$. In region IIa, the solution $\phi = \phi(x, t) \in C^1$ satisfies $\partial_t \phi > 0$, $\partial_x \phi < 0$, $\phi > \phi_G^* > \phi_{\rm infl}$ and is described by strictly concave characteristics emanating tangentially from the bottom discontinuity $x = b(t)$ for $t_1 \leq t \leq t_2$.*

Proof. For every $\bar t \in (t_1, t_2)$ let $(X(\bar t), \bar t) = (b(\bar t), \bar t)$ be the initial point at the bottom discontinuity $x = b(t)$ for a characteristic having the starting value $\Phi(\bar t) = \phi_b^*(\bar t)$. Since (12), Lemma 3 (i) and (34) give, in turn,

$$X'(\bar t) = -f'(\Phi(\bar t)) = -f'(\phi_b^*(\bar t)) = -S\big(\phi_b(\bar t), \phi_b^*(\bar t)\big) = b'(\bar t),$$

the characteristic emanates tangentially from the bottom (contact) discontinuity for increasing $t \geqslant \bar t$. The increase of $\Phi(t)$ implies, together with (13) and $\Phi(t) \geq \phi_b^*(t) > \phi_{\rm infl}$, that the characteristics are concave. Since the bottom discontinuity is convex

and the emanating characteristics are concave, the latter go into region IIa. Assume first that $q > 0$. System (16) becomes with $\tau = \bar{t}$, $\xi = b(\bar{t})$ and $\varphi = \phi_b^*(\bar{t})$:

$$f(\phi)(p+qx)^{1/q} = g(\bar{t}), \quad \text{where } g(\bar{t}) := f(\phi_b^*(\bar{t}))\big(p+qb(\bar{t})\big)^{1/q} \tag{40}$$

$$t = \bar{t} + \big(p+qb(\bar{t})\big) f(\phi_b^*(\bar{t}))^q \int_{\phi_b^*(\bar{t})}^{\phi} \frac{\mathrm{d}\Phi}{f(\Phi)^{1+q}}. \tag{41}$$

Eliminating $\bar{t}$, we obtain a relation between ϕ, x and t. We have

$$g'(\bar{t}) = f'\big(\phi_b^*(\bar{t})\big)(\phi_b^*)'(\bar{t})\big(p+qb(\bar{t})\big)^{1/q} + f\big(\phi_b^*(\bar{t})\big)\big(p+qb(\bar{t})\big)^{1/q-1} b'(\bar{t}) > 0, \tag{42}$$

since $f'(\phi_b^*(\bar{t})) < 0$ and $(\phi_b^*)'(\bar{t}) = (\mathrm{d}\phi_b^*/\mathrm{d}\phi_b)\phi_b'(\bar{t}) < 0$ by Lemma 3. Hence, the inverse of g exists, so $\bar{t}$ is an implicitly defined function of (ϕ, x) in region IIa by (40): $\bar{t} = \bar{t}(\phi, x) := g^{-1}\big(f(\phi)(p+qx)^{1/q}\big)$. This can be substituted into (41) so that

$$t = \bar{t}(\phi, x) + (p+qx) f(\phi)^q \int_{\phi_b^*(\bar{t}(\phi,x))}^{\phi} \frac{\mathrm{d}\Phi}{f(\Phi)^{1+q}} =: F(\phi, x). \tag{43}$$

The implicit function theorem states that (43) defines a continuously differentiable function $\phi = \phi(x,t)$ in a neighbourhood of (ϕ, x) where $\partial_\phi F \neq 0$. For the ease of notation, we set $z := \phi_b^*(\bar{t}(\phi, x))$ and $a(x) := p + qx$, and calculate

$$\begin{aligned}
\frac{\partial F}{\partial \phi} &= \frac{\partial \bar{t}}{\partial \phi} + a(x)\left(q f(\phi)^{q-1} f'(\phi) \int_z^{\phi} \frac{\mathrm{d}\Phi}{f(\Phi)^{1+q}} + f(\phi)^q \left(\frac{1}{f(\phi)^{1+q}} - \frac{(\phi_b^*)'(\bar{t})}{f(z)^{1+q}} \frac{\partial \bar{t}}{\partial \phi} \right) \right) \\
&= \frac{\partial \bar{t}}{\partial \phi} \left(1 - \frac{a(x) f(\phi)^q (\phi_b^*)'(\bar{t})}{f(z)^{1+q}} \right) + a(x)\left(q f(\phi)^{q-1} f'(\phi) \int_z^{\phi} \frac{\mathrm{d}\Phi}{f(\Phi)^{1+q}} + \frac{1}{f(\phi)} \right).
\end{aligned}$$

We shall first rewrite the term $\partial \bar{t}/\partial \phi$. By (34) and (35) (recall $\phi_b(t) \geq \phi_{\max}^{**}$), we have $b'(t) = -f'(z)$, and by (40) we can rewrite (42) as follows

$$\begin{aligned}
g'(\bar{t}) &= f'(z)(\phi_b^*)'(\bar{t}) a(b(\bar{t}))^{1/q} - f(z) a(b(\bar{t}))^{1/q-1} f'(z) \\
&= f'(z)(\phi_b^*)'(\bar{t}) \frac{f(\phi) a(x)^{1/q}}{f(z)} - f(z) \frac{f(\phi)^{1-q} a(x)^{1/q-1}}{f(z)^{1-q}} f'(z) \\
&= \frac{f'(z) a(x)^{1/q-1}}{f(z) f(\phi)^{q-1}} \big(a(x) f(\phi)^q (\phi_b^*)'(\bar{t}) - f(z)^{q+1} \big).
\end{aligned}$$

Differentiating $g(\bar{t}) = f(\phi) a(x)^{1/q}$, we get

$$\frac{\partial \bar{t}}{\partial \phi} = \frac{f'(\phi) a(x)^{1/q}}{g'(\bar{t})} = \frac{f'(\phi) a(x) f(z) f(\phi)^{q-1}}{f'(z)\big(a(x) f(\phi)^q (\phi_b^*)'(\bar{t}) - f(z)^{q+1}\big)}.$$

Now we get

$$\begin{aligned}
\frac{\partial F}{\partial \phi} &= -\frac{a(x) f'(\phi) f(\phi)^{q-1}}{f'(z) f(z)^q} + a(x)\left(q f(\phi)^{q-1} f'(\phi) \int_z^{\phi} \frac{\mathrm{d}\Phi}{f(\Phi)^{q+1}} + \frac{1}{f(\phi)} \right) \\
&= a(x) f(\phi)^{q-1} \left(q f'(\phi) \int_z^{\phi} \frac{\mathrm{d}\Phi}{f(\Phi)^{q+1}} + \frac{1}{f(\phi)^q} - \frac{f'(\phi)}{f'(z) f(z)^q} \right).
\end{aligned}$$

Observe that for $\phi_{\mathrm{infl}} \leqslant z < \phi$, we have $f'(\Phi) < f'(\phi)$ for $z \leqslant \Phi < \phi$. Therefore,

$$q f'(\phi) \int_z^{\phi} \frac{\mathrm{d}\Phi}{f(\Phi)^{q+1}} \geq q \int_z^{\phi} \frac{f'(\Phi)\mathrm{d}\Phi}{f(\Phi)^{q+1}} = \frac{1}{f(z)^q} - \frac{1}{f(\phi)^q}. \tag{44}$$

Consequently,

$$\frac{\partial F}{\partial \phi} \geq a(x) f(\phi)^{q-1} \left(\frac{1}{f(z)^q} - \frac{f'(\phi)}{f'(z) f(z)^q} \right) = \frac{a(x) f(\phi)^{q-1}}{f(z)^q} \left(1 - \frac{f'(\phi)}{f'(z)} \right) > 0, \tag{45}$$

since $f'(z) < f'(\phi) < 0$. Finally, we compute the partial derivatives of the solution. Differentiating $g(\bar{t}(\phi, x)) = f(\phi) a(x)^{1/q}$ with respect to x, we get

$$\frac{\partial \bar{t}}{\partial x} = \frac{f(\phi)(p + qx)^{1/q-1}}{g'(\bar{t})} > 0$$

and, since $(\phi_b^*)'(t) < 0$ (by $\mathrm{d}\phi^*/\mathrm{d}\phi < 0$ and the fact that $\phi_b(t)$ is increasing), we have

$$\frac{\partial F}{\partial x} = \frac{\partial \bar{t}}{\partial x} + q f(\phi)^q \int_z^\phi \frac{\mathrm{d}\Phi}{f(\Phi)^{1+q}} - \frac{a(x) f(\phi)^q (\phi_b^*)'(\bar{t})}{f(z)^{1+q}} \frac{\partial \bar{t}}{\partial x} > 0, \tag{46}$$

so differentiating $F(\phi, x) = t$ (43) yields $\partial_t \phi = 1/\partial_\phi F > 0$ and $\partial_x \phi = -\partial_x F / \partial_\phi F < 0$.

To prove the lemma in the case $q = 0$, it suffices to see that the key inequalities above hold also when $q \to 0^+$. The inequality (45) is clearly true. Furthermore,

$$\begin{aligned} \frac{\partial \bar{t}}{\partial x} &= \frac{f(\phi) a(x)^{1/q-1}}{g'(\bar{t})} = \frac{f(\phi) a(x)^{1/q-1} f(z) f(\phi)^{q-1}}{f'(z) a(x)^{1/q-1} (a(x) f(\phi)^q (\phi_b^*)'(\bar{t}) - f(z)^{q+1})} \\ &= \frac{f(z) f(\phi)^q}{f'(z)(a(x) f(\phi)^q (\phi_b^*)'(\bar{t}) - f(z)^{q+1})} \overset{q \to 0^+}{\longrightarrow} \frac{f(z)}{f'(z)(p\,(\phi_b^*)'(\bar{t}) - f(z))} > 0. \end{aligned}$$

Hence, (46) is also true as $q \to 0^+$. ∎

Case L: The upper boundary discontinuity of region IIa. The remaining piece of boundary of region IIa is the upper shock wave $x = h(t)$ for $t_{2.5} < t < t_3$.

LEMMA 9. *The discontinuity $x = h(t)$, $t_{2.5} \leq t \leq t_3$, is a shock wave that satisfies the jump condition (8), the entropy condition (9), $h'(t) < 0$ and $h''(t) > 0$. If $t_2 = t_{2.5}$, then there is a jump in the slope of the sediment level at $t = t_2$: the downwards speed of the sediment level decreases. If $t_2 < t_{2.5}$, then $h(t) \in C^1$ for $t > 0$. The solution ϕ is zero for $x > h(t)$ and just below the shock the solution values are given by the increasing smooth function $\phi_h(t)$, whose connection to $h(t)$ is given by (29).*

Proof. The function $h(t)$ satisfies the jump condition (29), where the values $\phi_h(t)$ just below the shock are those carried by the characteristics that originate tangentially from the bottom discontinuity. The shock satisfies the entropy conditions; see (30). According to Lemma 7, the solution in region I satisfies $\phi < \phi_G < \phi_{\mathrm{infl}}$. In particular, the concentration values along the upper and lower discontinuities satisfy $\phi_h(t), \phi_b(t) < \phi_G < \phi_{\mathrm{infl}}$ for $t < t_2$. Lemma 3 (i) and (iii) then imply that the values just below $x = b(t)$ satisfy $\phi_b^*(t) > \phi_G^* > \phi_{\mathrm{infl}}$ for $t_1 \leq t \leq t_{2.5}$. These values are the starting values for each tangentially emanating characteristic. Since ϕ increases along every characteristic we also have $\phi_h(t) > \phi_G^* > \phi_{\mathrm{infl}}$ for $t_{2.5} < t < t_3$. If $t_2 = t_{2.5}$, then $\phi_h(t_{2.5}^-) < \phi_{\mathrm{infl}} < \phi_h(t_{2.5}^+)$, wherefore the decreasing settling velocity function implies $h'(t_2^-) = -v(\phi_h(t_2^-)) < -v(\phi_h(t_2^+)) = h'(t_2^+) < 0$, so there is a jump in the slope of the sediment level at $t = t_{2.5}$. If $t_2 < t_{2.5}$, then $\phi_h(t)$ is continuous at $t = t_{2.5}$. As $t \nearrow t_3$, we have $\phi_h(t) \nearrow \phi_{\max}$ and $h'(t) \searrow 0$ by (29), and finally $h'(t) = 0$ for $t \geqslant t_3$.

It remains to prove that $h(t)$ is convex. Once we have obtained that $\phi_h'(t) > 0$ for $t_{2.5} < t < t_3$, the convexity follows by differentiation of the jump condition (29):

$$h''(t) = -v'\big(\phi_h(t)\big)\phi_h'(t) > 0, \quad t_2 < t < t_3. \tag{47}$$

The solution in region IIa is given implicitly by Equation (43). Inserting $x = h(t)$ and $\phi = \phi_h(t)$, the equation becomes $t = F(\phi_h(t), h(t))$, which we can differentiate to get

$$\phi_h'(t) = \frac{1 - \partial_x F\big(\phi_h(t), h(t)\big) h'(t)}{\partial_\phi F\big(\phi_h(t), h(t)\big)} = \frac{1 + \partial_x F\big(\phi_h(t), h(t)\big) v(\phi_h(t))}{\partial_\phi F\big(\phi_h(t), h(t)\big)} > 0, \tag{48}$$

since $\partial_\phi F > 0$ by (45) and $\partial_x F > 0$ by (46). ∎

The straight line of continuity $x = \ell(t)$, which is the leftmost characteristic carrying the maximum volume fraction $\phi_{\max}$, is $x = b(t_1) + f'(\phi_{\max})(t - t_1)$. Recall that $t_1 = 0$ if $\phi_0 = \phi_{\max}^{**}$. Since the total mass is the same at $t = 0$ and $t = t_3$, we have

$$\phi_0 \int_0^1 A(x)\,\mathrm{d}x = \phi_{\max} \int_0^{\ell(t_3)} A(x)\,\mathrm{d}x. \tag{49}$$

For the function $A(x)$ given by (5), it is straightforward to obtain an explicit expression for $\ell(t_3)$. This principle can also be used for the numerical determination of $h(t)$ for $t_{2.5} \le t < t_3$, which we have utilized in the figures.

REMARK 1. *In the well-known special case $A = \text{const}$. (see e.g. [10]), (12) implies that the characteristics are straight lines along which ϕ is constant. Region I then has the constant concentration ϕ_0 and $x = h(t)$ is a straight line for $0 \le t \le t_{2.5} = t_3$. Region IIa is empty and in Case L there is a shock wave between regions I and III with the velocity $S(\phi_0, \phi_{\max})$ for $0 \le t \le t_{2.5} = t_3$, after which the solution is stationary.*

4.3. Case H: $\phi_{\mathrm{infl}} \leqslant \phi_0 < \phi_{\max}$. The solution is shown in Figure 5 (left column).

Case H: The solution in regions I and III. Since ϕ increases along each characteristic that starts from $t = 0$, the solution in region I is greater than $\phi_0 \geqslant \phi_{\mathrm{infl}}$ and the characteristics are concave; see (13). The expressions (26) and (24) give that Lemma 4 holds with $Q'(\phi) > 0$ for all ϕ in region I (for $q = 0$ this is always true by Lemma 5). The slope of each characteristic is initially $-f'(\phi_0) > 0$ and then decreases with the lower bound $-f'(\phi_{\max}) \ge 0$. From the bottom boundary and for $t > 0$, there are characteristics emanating into region III all having the constant slope $-f'(\phi_{\max})$. If $f'(\phi_{\max}) = 0$, then region III is empty.

Case H: The solution in region IIb. Region IIb of Figure 5 is bounded by the sediment level $x = h(t)$ (to be determined), the concave characteristic emanating initially from the bottom, i.e. $(x, t) = (0^+, 0)$, having the initial slope $-f'(\phi_0) > -f'(\phi_{\max})$, and the bottom straight-line characteristic $x = \ell(t) = -f'(\phi_{\max})t$.

LEMMA 10. *In region IIb, the solution $\phi = \phi(x, t) \in C^1$ satisfies $\partial_t \phi > 0$, $\partial_x \phi < 0$ and is described by a fan of strictly concave characteristics all emanating from the origin $(x, t) = (0, 0)$ with the initial values in the interval $(\phi_0, \phi_{\max})$.*

Proof. The fan of characteristics emanating from the origin have the initial slopes $X'(0) = -f'(\varphi)$, $\varphi \in (\phi_0, \phi_{\max})$. For $q > 0$, system (16) with $\xi = 0$ and $\tau = 0$ is

$$t = (p + qx) f(\phi)^q \int_\varphi^\phi \frac{\mathrm{d}\Phi}{f(\Phi)^{1+q}}, \qquad \frac{f(\phi)}{f(\varphi)} = \left(\frac{p}{p + qx}\right)^{1/q}. \tag{50}$$

Since $f|_{(\varphi, \phi_{\max})}$ is decreasing, it is invertible. Hence, the second equation of (50) gives $\varphi = \varphi(\phi, x) := f^{-1}(Z(\phi, x))$, where $Z(\phi, x) := f(\phi)\,(1 + qx/p)^{1/q}$, which we substitute into the first equation:

$$t = (p + qx) f(\phi)^q \int_{\varphi(\phi, x)}^\phi \frac{\mathrm{d}\Phi}{f(\Phi)^{1+q}} =: \tilde{F}(\phi, x). \tag{51}$$

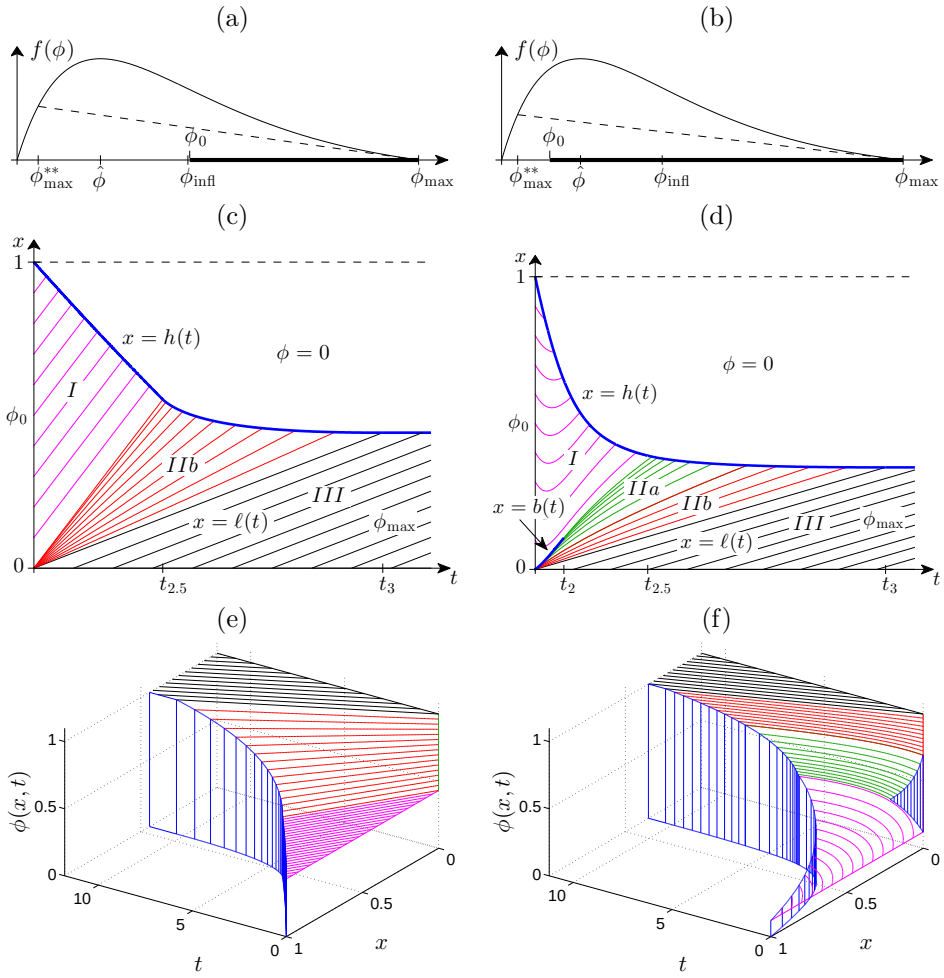

FIG. 5. (a, c, e) *Case H:* $\phi_{\rm infl} \leqslant \phi_0 < \phi_{\max}$ *with* $\phi_0 = 0.43$, $p = 9.5$, $r_{\rm V} = 4.7$, $\phi^{**}_{\max} = 0.0524$, $\hat\phi = 0.208$ *and* $\phi_{\rm infl} = 0.426$. *The only discontinuity is the upper shock wave* $x = h(t)$, $t \geq 0$, *with* $h \in C^1$. (b, d, f) *Case M:* $\phi^{**}_{\max} \leqslant \phi_0 < \phi_{\rm infl}$ *with* $\phi_0 = 0.12$, $p = 1/6$, $r_{\rm V} = 5$, $r_{\rm V} = 4$, $\phi^{**}_{\max} = 0.0398$, $\hat\phi = 0.196$ *and* $\phi_{\rm infl} = 0.4$.

This is an implicit equation for the smooth function $\phi = \phi(x,t)$ in region IIb if $\partial_\phi \tilde F \neq 0$ holds there. Differentiating $f(\varphi(\phi,x)) = Z(\phi,x)$ and using (50), we get

$$\frac{\partial\varphi}{\partial\phi} = \frac{\partial_\phi Z(\phi,x)}{f'(\varphi)} = \frac{f'(\phi)(1+qx/p)^{1/q}}{f'(\varphi)} = \frac{f'(\phi)f(\varphi)}{f'(\varphi)f(\phi)}.$$

Hence, using $f'(\varphi) \leq f'(\Phi) \leq f'(\phi) < 0$ for $\varphi \leq \Phi \leq \phi$ and (44), we have

$$\begin{aligned}\frac{1}{p+qx}\frac{\partial\tilde F}{\partial\phi} &= qf(\phi)^{q-1}f'(\phi)\int_{\varphi(\phi,x)}^{\phi}\frac{\mathrm{d}\Phi}{f(\Phi)^{1+q}} + f(\phi)^q\left(\frac{1}{f(\phi)^{1+q}} - \frac{1}{f(\varphi)^{1+q}}\frac{\partial\varphi}{\partial\phi}\right)\\ &\geq f(\phi)^{q-1}q\int_{\varphi(\phi,x)}^{\phi}\frac{f'(\Phi)\mathrm{d}\Phi}{f(\Phi)^{1+q}} + f(\phi)^q\left(\frac{1}{f(\phi)^{1+q}} - \frac{f'(\phi)}{f(\varphi)^q f'(\varphi)f(\phi)}\right)\\ &= \frac{f(\phi)^{q-1}}{f(\varphi)^q}\left(1 - \frac{f'(\phi)}{f'(\varphi)}\right) > 0. \qquad (52)\end{aligned}$$

Moreover, $\partial_x \varphi = \partial_x Z(\phi, x)/f'(\varphi) = (1 + qx/p)^{1/q-1}/(pf'(\varphi)) < 0$ implies that

$$\frac{\partial \tilde{F}}{\partial x} = qf(\phi)^q \int_{\varphi(\phi,x)}^{\phi} \frac{\mathrm{d}\Phi}{f(\Phi)^{1+q}} - \frac{(p+qx)f(\phi)^q}{f(\varphi(\phi,x))^{1+q}} \frac{\partial \varphi}{\partial x} > 0. \tag{53}$$

Differentiating (51), we get $\partial_t \phi > 0$ and $\partial_x \phi < 0$ as in the proof of Lemma 8. The case $q = 0$ can again be obtained as the limit $q \to 0^+$. It is easy to verify that the strict inequalities of (52) and (53) still hold. ∎

Case H: The upper boundary of region IIb. The shock wave $x = h(t)$ for $t_{2.5} < t < t_3$ satisfies (29) where $\phi_h(t)$ are the solution values just below the shock wave. The final sediment level can be obtained with (49) and hence the time point t_3. From the construction, this concentration reaches $\phi_{\max}$ at $t = t_3$, and then $h'(t_3) = -v(\phi_{\max}) = 0$. That $h(t)$ is convex for $t_{2.5} < t < t_3$ can be proved in the same way as for the shock above region IIa. Inserting $x = h(t)$ and $\phi = \phi_h(t)$ into (51), the equation becomes $t = \tilde{F}(\phi_h(t), h(t))$. Differentiating this we get (48) with F replaced by $\tilde{F}$, which is true since $\partial_\phi \tilde{F} > 0$ and $\partial_x \tilde{F} > 0$ by (52) and (53). Eventually, h is strictly convex by (47).

Remark 2. *In this special case when A is constant, region I has the constant solution ϕ_0 and region IIa is empty. In both Cases H and M, region IIb is filled with an expansion wave with straight characteristics. Above region IIb, the shock $x = h(t)$ is convex, otherwise it has constant velocity. In Case H, there is no bottom discontinuity, while there is one in Case M between regions I and IIb having the velocity $S(\phi_0, \phi_0^*)$.*

4.4. Case M: $\phi_{\max}^{**} < \phi_0 < \phi_{\mathrm{infl}}$. The solution is shown in Figure 5 (right column) in the subcase when the bottom discontinuity $x = b(t)$ does not reach the upper shock wave $x = h(t)$. As in Case L, there exists a second subcase where both discontinuities intersect at $t = t_{2.5}$. These two subcases correspond qualitatively to the numerical solutions of [7, Figs 2 (c) and (e)]. The qualitatively different solutions in the four regions correspond to the constructions in the previous sections. In addition, the boundaries of the regions possess no new phenomena.

4.5. Main theorem. We summarize here the main properties of the solution. All details are contained in the lemmas above.

Theorem 1. *The entropy solution $\phi = \phi(x,t)$ of (1), where $A(x)$ is given by (5) with $p, q > 0$ or $p > 0$ and $q \to 0^+$, is piecewise smooth, has a shock wave $x = h(t)$, $t \geq 0$, declining from the top, and the following properties:*

(i) *A contact discontinuity $x = b(t)$, $0 \leq t \leq t_2$, rises from the bottom if and only if $0 < \phi_0 < \phi_{\mathrm{infl}}$ (Cases L and M). The functions h and b are convex and smooth, except if $t_2 = t_{2.5}$, which means that the two shock waves intersect; then h' has a discontinuity at $t = t_{2.5}$.*

(ii) *The solution satisfies, in the weak sense, $\partial_t \phi > 0$ and $\partial_x \phi < 0$ with the following exceptions: the regions with $\phi = 0$ above $x = h(t)$ and $\phi = \phi_{\max}$ in region III; and if $q = 0$, then $\partial_t \phi > 0$ and $\partial_x \phi = 0$ in region I.*

(iii) *The solution in region I is given by (22).*

(iv) *Region IIa is empty if $\phi_{\mathrm{infl}} < \phi_0 < \phi_{\max}$ (Case H). Otherwise, the solution in region IIa satisfies $\phi > \phi_{\mathrm{infl}}$ and is described by strictly concave characteristics emanating tangentially from the bottom discontinuity $x = b(t)$ for $t_1 \leq t \leq t_2$.*

(v) *Region IIb is empty if $\phi_0 \leq \phi_{\max}^{**}$ (Case L). Otherwise region IIb is filled with a fan of concave characteristics emanating from the origin $(x,t) = (0,0)$ with values in the interval $(\phi_0^*, \phi_{\max})$ if $\phi_{\max}^{**} < \phi_0 < \phi_{\mathrm{infl}}$ (Case M), and in $(\phi_0, \phi_{\max})$ if $\phi_{\mathrm{infl}} \leq \phi_0 < \phi_{\max}$ (Case H).*

5. Conclusions. We have solved the problem (1) for cross-sectional areas A of the shape (5) with $p > 0$ and $q \geq 0$ and for unimodal flux functions f having at most one inflexion point to the right of its maximum point. Three main cases appear depending on the initial concentration ϕ_0. The well-known special case of a constant A is commented on in each case; all characteristics are straight lines carrying values of constant ϕ and the solution in region I is constant. Then the sinking sediment level, i.e. the upper shock wave $x = h(t)$, has a constant speed, which has for a century been utilized for batch test measurement and thereby determination of one point of the flux function f. The main features in the case $A' > 0$ (in comparison to the case $A' = 0$) are that the characteristics are non-straight lines, the possible discontinuity from bottom may disappear before reaching the sediment level (see Figures 3 (c, e), and 5 (d, f)). Furthermore, we mention that for downward-contracting vessels, the solutions constructed by Anestis [1] are limited to the convex flux $f(\phi) = \phi(1 - \phi)$ and a conical vessel ($m = 1/q = 2$, see Section 2.1). The present work leads to the same results as [1] for this special scenario. The decisive difference of our approach is, however, that our implementation of the method of characteristics (see Section 4.1) is based on integrals with respect to ϕ, while the treatment in [1] is based on integrations with respect to f, which is feasible only if f is invertible (at least in a piecewise sense).

An important observation is that the concentration $\phi_h(t)$ below the convex sediment level increases with time, implying the possibility of developing new methods of determining the flux function for those concentrations. For example, in the case $q = 0$, i.e. when $A(x) = \mathrm{e}^{(x-1)/p}$, the formula (28) with $x = h(t)$ can be differentiated to yield $\phi_h'(t) = f(\phi_h(t))/p$. Hence, a part of the flux function f can be estimated if the concentration along the sediment level can be measured as a function of time (and differentiated). The authors will expand on the application of the present results to the problem of flux identification in future work.

REFERENCES

[1] G. Anestis, *Eine eindimensionale Theorie der Sedimentation in Absetzbehältern veränderlichen Querschnitts und in Zentrifugen*, PhD thesis, TU Vienna, Austria, 1981.

[2] G. Anestis and W. Schneider, *Application of the theory of kinematic waves to the centrifugation of suspensions*, Ing. arch, 53 (1983), pp. 399–407.

[3] D. P. Ballou, *Solutions to nonlinear hyperbolic Cauchy problems without convexity conditions*, Trans. Amer. Math. Soc., 152 (1970), pp. 441–460.

[4] E. S. Benilov, C. P. Cummins, and W. T. Lee, *Why do bubbles in Guinness sink?*, Am. J. Phys., 81 (2013), p. 88.

[5] F. Betancourt, R. Bürger, S. Diehl, and C. Mejías, *Advanced methods of flux identification for clarifier–thickener simulation models*, Minerals Eng., 63 (2014), pp. 2–15.

[6] U. Borgmann and W. P. Norwood, *Sediment toxicity testing using large water–sediment ratios: an alternative to water renewal*, Environm. Pollution, 106 (1999), pp. 333–339.

[7] R. Bürger, J. J. R. Damasceno, and K. H. Karlsen, *A mathematical model for batch and continuous thickening of flocculated suspensions in vessels with varying cross-section*, Int. J. Miner. Process., 73 (2004), pp. 183–208.

[8] R. Bürger and S. Diehl, *Convexity-preserving flux identification for scalar conservation laws modelling sedimentation*, Inverse Problems, 29 (2013), p. 045008.

[9] R. Bürger, K. H. Karlsen, and J. D. Towers, *A model of continuous sedimentation of flocculated suspensions in clarifier-thickener units*, SIAM J. Appl. Math., 65 (2005), pp. 882–940.

[10] M. C. Bustos, F. Concha, R. Bürger, and E. M. Tory, *Sedimentation and Thickening: Phenomenological Foundation and Mathematical Theory*, Kluwer Academic Publishers, Dordrecht, The Netherlands, 1999.

[11] J.-P. Chancelier, M. C. de Lara, and F. Pacard, *Analysis of a conservation PDE with discontinuous flux: A model of settler*, SIAM J. Appl. Math., 54 (1994), pp. 954–995.

[12] K.-S. Cheng, *Constructing solutions of a single conservation law*, J. Differ. Equat., 49 (1983),

pp. 344–358.
[13] J. Corberán and M. Gascón, *TVD schemes for the calculation of flow in pipes of variable cross-section*, Mathematical and Computer Modelling, 21 (1995), pp. 85–92.
[14] C. M. Dafermos, *Regularity and large time behaviour of solutions of conservation laws without convexity*, Proc. Roy. Soc. Edinburgh Sect. A, 99 (1985), pp. 201–239.
[15] S. Diehl, *A conservation law with point source and discontinuous flux function modelling continuous sedimentation*, SIAM J. Appl. Math., 56 (1996), pp. 388–419.
[16] S. Diehl, *Dynamic and steady-state behavior of continuous sedimentation*, SIAM J. Appl. Math., 57 (1997), pp. 991–1018.
[17] S. Diehl, *Estimation of the batch-settling flux function for an ideal suspension from only two experiments*, Chem. Eng. Sci., 62 (2007), pp. 4589–4601.
[18] S. Diehl, *Shock-wave behaviour of sedimentation in wastewater treatment: A rich problem*, in Analysis for Science, Engineering and Beyond, K. Åström, L.-E. Persson, and S. D. Silvestrov, eds., vol. 6 of Springer Proceedings in Mathematics, 2012, pp. 175–214.
[19] P. Grassia, S. P. Usher, and P. J. Scales, *Closed-form solutions for batch settling height from model settling flux functions*, Chem. Eng. Sci., 66 (2011), pp. 964–972.
[20] H. Holden and N. H. Risebro, *Front Tracking for Hyperbolic Conservation Laws*, Springer Berlin Heidelberg, 2011.
[21] H. Jiao, A. Wu, H. Wang, S. Zhong, R. Ruan, and S. Yin, *The solids concentration distribution in the deep cone thickener: A pilot scale test*, Korean J. Chem. Eng., 30 (2013), pp. 262–268.
[22] G. J. Kynch, *A theory of sedimentation*, Trans. Faraday Soc., 48 (1952), pp. 166–176.
[23] W. Liao, A. Tordeux, A. Seyfried, M. Chraibi, K. Drzycimski, X. Zheng, and Y. Zhao, *Measuring the steady state of pedestrian flow in bottleneck experiments*, Physica A: Stat. Mech. Applic., 461 (2016), pp. 248–261.
[24] M. Marsi and V. P. Evangelou, *Chemical and physical behavior of two kentucky soils: III. saturated hydraulic conductivity – imhoff cone test relationships*, J. Environm. Sci. Health. Part A: Environm. Sci. Eng. Toxicology, 26 (1991), pp. 1195–1215.
[25] O. A. Oleinik, *Uniqueness and stability of the generalized solution of the Cauchy problem for a quasi-linear equation*, Uspekhi Mat. Nauk, 14 (1959), pp. 165–170. Amer. Math. Soc. Trans. Ser. 2, 33, (1964), pp. 285–290.
[26] M. Poloni, D. Winterbone, and J. Nichols, *Comparison of unsteady flow calculations in a pipe by the method of characteristics and the two-step differential Lax-Wendroff method*, International Journal of Mechanical Sciences, 29 (1987), pp. 367–378.
[27] J. F. Richardson and W. N. Zaki, *Sedimentation and fluidization: part I.*, Trans. Instn. Chem. Engrs. (London), 32 (1954), pp. 35–53.
[28] T. Rupprecht, W. Klingsch, and A. Seyfried, *Influence of geometry parameters on pedestrian flow through bottleneck*, in Pedestrian and Evacuation Dynamics, Springer Science+Business Media, 2011, pp. 71–80.
[29] R. E. Sojka, D. L. Carter, and M. J. Brown, *Imhoff cone determination of sediment in irrigation runoff*, Soil Science Society of America Journal, 56 (1992), pp. 884–890.
[30] M. D. Thanh, *The Riemann problem for a nonisentropic fluid in a nozzle with discontinuous cross-sectional area*, SIAM J. Appl. Math., 69 (2009), pp. 1501–1519.
[31] H. M. Zhang, *New perspectives on continuum traffic flow models*, Networks Spatial Economics, 1 (2001), pp. 9–33.
[32] J. Zhang, D. Britto, M. Chraibi, R. Löhner, E. Haug, and B. Gawenat, *Quantitative validation of PEDFLOW for description of unidirectional pedestrian dynamics*, Transportation Research Procedia, 2 (2014), pp. 733–738.
[33] J. Zhang and A. Seyfried, *Quantification of bottleneck effects for different types of facilities*, Transportation Research Procedia, 2 (2014), pp. 51–59.